The International Journal of Biochemistry & Cell Biology 45 (2013) 1878–1885

Contents lists available at SciVerse ScienceDirect

The International Journal of Biochemistry & Cell Biology

journal homepage: www.elsevier.com/locate/biocel

Mechanism of the dehydrogenase reaction of DmpFG and analysis of inter-subunit channeling efficiency and thermodynamic parameters in the overall reaction

Natalie E. Smith[a], Wan Jun Tie[a], Gavin R. Flematti[a], Keith A. Stubbs[a], Ben Corry[b], Paul V. Attwood[a], Alice Vrielink[a,*]

[a] School of Chemistry and Biochemistry, University of Western Australia, 35 Stirling Highway, Crawley, WA 6009, Australia
[b] Research School of Biology, Australian National University, Acton, ACT 0200, Australia

ARTICLE INFO

Article history:
Received 18 April 2013
Received in revised form 23 May 2013
Accepted 27 May 2013
Available online 3 June 2013

Keywords:
Enzyme activity
Substrate channeling
Thermodynamic activation parameters
Allosteric interaction

ABSTRACT

The bifunctional, microbial enzyme DmpFG is comprised of two subunits: the aldolase, DmpG, and the dehydrogenase, DmpF. DmpFG is of interest due to its ability to channel substrates between the two spatially distinct active sites. While the aldolase is well studied, significantly less is known about the dehydrogenase. Steady-state kinetic measurements of the reverse reaction of DmpF confirmed that the dehydrogenase uses a ping-pong mechanism, with substrate inhibition by acetyl CoA indicating that NAD^+/NADH and CoA/acetyl CoA bind to the same site in DmpF. The K_m of DmpF for exogenous acetaldehyde as a substrate was 23.7 mM, demonstrating the necessity for the channel to deliver acetaldehyde directly from the aldolase to the dehydrogenase active site. A channeling assay on the bifunctional enzyme gave an efficiency of 93% indicating that less than 10% of the toxic acetaldehyde leaks out of the channel into the bulk media, prior to reaching the dehydrogenase active site. The thermodynamic activation parameters of the reactions catalyzed by the aldolase, the dehydrogenase and the DmpFG complex were determined. The Gibb's free energy of activation for the dehydrogenase reaction was lower than that obtained for the full DmpFG reaction, in agreement with the high k_{cat} obtained for the dehydrogenase reaction in isolation. Furthermore, although both the DmpF and DmpG reactions occur with small, favorable entropies of activation, the full DmpFG reaction occurs with a negative entropy of activation. This supports the concept of allosteric structural communication between the two enzymes to coordinate their activities.

1. Introduction

4-Hydroxy-2-ketovalerate aldolase–aldehyde dehydrogenase (acylating) (DmpFG) is a bifunctional enzyme from *Pseudomonas* sp. strain CF600 and is composed of two subunits DmpG and DmpF. DmpG and DmpF, as the penultimate enzymes in the meta-cleavage pathway of catechol, (Powlowski et al., 1993; Shingler et al., 1992) function to convert 4-hydroxy-2-ketovalerate (HKV) to pyruvate and acetyl CoA (Fig. 1). The intermediate formed in this reaction, acetaldehyde, is toxic to the bacteria as it rapidly reacts with nucleophiles such as cysteine, to form covalent adducts (Brecher et al., 1997). As such, release into the bulk media of the cell would not be advantageous to the organism. When the crystal structure of DmpFG was determined a 29 Å long, water filled channel was observed linking the aldolase active site in DmpG to the dehydrogenase active site in DmpF supporting the possibility that DmpFG used substrate channeling to transport its intermediate (Manjasetty et al., 2003). Buried channels have been observed for other bifunctional enzymes as a means of channeling volatile or reactive intermediates between distant active sites (Chaudhuri et al., 2001; Darnault et al., 2003; Doukov et al., 2002; Drennan et al., 2001; Hyde et al., 1988; Kim et al., 1996; Knighton et al., 1994; Krahn et al., 1997; Larsen et al., 1999; Muchmore et al., 1998; Smith et al., 1994; Thoden et al., 1997). This mechanism of substrate channeling is further advantageous as it isolates the intermediate from the bulk solvent whilst increasing reaction rates and efficiencies (Huang et al., 2001; Milani et al., 2003; Miles et al., 1999; Weeks et al., 2006).

DmpG or HKV aldolase, is a Class II aldolase which uses a Mn^{2+} ion to catalyze the aldol cleavage of HKV to acetaldehyde with the release of pyruvate. A previous study has found that the activity of DmpG, was stimulated by the addition of both Mn^{2+} and NADH to the reaction mixture (Powlowski et al., 1993). In fact Mn^{2+} (1 mM) stimulated aldolase activity by six to eightfold. The aldolase

* Corresponding author. Tel.: +61 8 6488 3162; fax: +61 8 6488 1001.
E-mail address: alice.vrielink@uwa.edu.au (A. Vrielink).

1357-2725/$ – see front matter © 2013 Elsevier Ltd. All rights reserved.
http://dx.doi.org/10.1016/j.biocel.2013.05.028

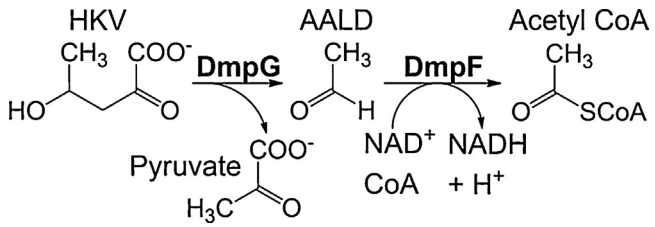

Fig. 1. The reaction pathway catalyzed by DmpFG. 4-Hydroxy-2-ketovalerate (HKV) is converted to acetaldehyde (AALD) and pyruvate. AALD is then transported through the channel to DmpF where it is converted to acetyl CoA with the concomitant conversion of NAD^+ to NADH.

exhibited the highest activity in the pH range 8.5–9.0 and the lowest activity was observed at pH 6.5 (Powlowski et al., 1993).

Two main classes of ALDHs are known; phosphorylating and non-phosphorylating (Feldman and Weiner, 1972; Racker and Krimsky, 1952; Segal and Boyer, 1953). In both cases the reaction mechanism leads to the formation of a thiohemiacetal intermediate. The reaction proceeds with the nucleophilic attack of the active site cysteine residue on the carbonyl carbon of the aldehyde substrate to form a thiohemiacetal intermediate. Subsequent hydride transfer to NAD^+ results in the formation of a thioacyl-enzyme intermediate. In non-phosphorylating ALDHs the thioacyl-enzyme intermediate undergoes nucleophilic attack either by water (CoA-independent/hydrolytic) or CoA (CoA-dependent/acylating). DmpF is a non-phosphorylating CoA-dependent ALDH. While there have been extensive structural and mechanistic studies of non-phosphorylating CoA-independent ALDHs (Ahvazi et al., 2000; Cobessi et al., 2000; D'Ambrosio et al., 2006; Farres et al., 1995; Liu et al., 1997; Steinmetz et al., 1997; Talfournier et al., 2009; Vedadi and Meighen, 1997; Wang and Weiner, 1995; Zhang et al., 1999), less is known about the CoA-dependent ALDHs. The structures of only two non-phosphorylating CoA-dependent acylating ALDHs have been characterized: DmpF, as part of the DmpFG complex (Manjasetty et al., 2003) and methylmalonate–semialdehyde dehydrogenase from *Bacillus subtilis* (Dubourg et al., 2004). Interestingly, DmpF is not structurally related to methylmalonate–semialdehyde dehydrogenase but shares similarities with glyceraldehyde-3-phosphate dehydrogenase, which is a phosphorylating dehydrogenase (Cobessi et al., 1999; Hadfield et al., 1999; Vellieux et al., 1993), suggesting that it belongs to a third class of ALDHs.

Similar to the aldolase DmpG it was found that the activity of the dehydrogenase DmpF increased from pH 6.5 to 8.5 (Powlowski et al., 1993). The aldehyde and nucleotide specificity of DmpF were investigated showing that DmpF could react with a series of aldehydes including acetaldehyde, propionaldehyde, butyraldehyde, isobutyraldehyde and formaldehyde and that $NADP^+$ could substitute for NAD^+ in this reaction. No metals stimulated the activity of DmpF (Powlowski et al., 1993). More recently, K_m values were obtained for CoA (87 μM) and NAD^+ (156 μM) in DmpF, however these studies were carried out using exogenous acetaldehyde under non-saturating conditions (38.4 mM) and no k_{cat} values were obtained (Lei et al., 2008).

The crystal structure of DmpFG in the presence of the cofactor revealed a Rossmann fold binding site for NAD^+ in DmpF however the binding site for CoA was not identified (Manjasetty et al., 2003; Sohling and Gottschalk, 1993). It has been suggested that DmpF undergoes a ping-pong mechanism where NAD^+ and acetaldehyde bind first and NADH must be released before CoA can bind in the active site (Powlowski et al., 1993). The presence of a shared binding site for the two cofactors has been supported by hydrogen–deuterium exchange experiments (Lei et al., 2008). In addition, during the purification of DmpFG, the enzyme could be eluted from an NAD^+ affinity column using either NAD^+ or CoA, further suggesting a common binding site. Furthermore, CoA was found to inhibit the enzyme, and this inhibition could be reversed by the addition of dithiothreitol (DTT) (Lei et al., 2008). Finally, inhibition by CoA could be prevented by pre-incubation of the protein with NAD^+, again implying competition for a shared binding site (Lei et al., 2008). While the crystal structure of DmpFG has been determined (Manjasetty et al., 2003), kinetic characterization of the bifunctional enzyme complex has not been rigorously performed. Little is known about the binding order and rate constants of the dehydrogenase, DmpF. As DmpFG is a bifunctional enzyme understanding how DmpF functions as an individual enzyme and as part of the DmpFG complex as a whole is important to allow increased applications for this class of aldolase–dehydrogenase enzymes for the synthesis of specific chemical products. To further our understanding of this bifunctional enzyme, we characterized the dehydrogenase, DmpF, in the context of the full DmpFG reaction and subsequently assayed it independently in both the forward and the reverse direction. We also investigated the channeling of acetaldehyde through this enzyme complex.

2. Methods

2.1. Synthesis of 4-hydroxy-2-ketovalerate

4-Methyl-2-oxobutyrolactone was synthesized as described by Rossi and Schinz yielding a thick brown oil (Rossi and Schinz, 1948). Purification of the butyrolactone was achieved using a silica chromatography column and hexane/EtOAc (60:40) as the mobile phase. The solvent was removed under reduced pressure yielding a white crystalline solid. The product was further purified by HPLC (Hewlett Packard 1050) using an Apollo C18 column (250 mm × 10 mm, 5 μm, Grace Davison Discovery Sciences) and a gradient of 1–30% acetonitrile with 0.1% TFA/H_2O over 30 min and a flow rate of 4 ml/min. Fractions shown to contain the lactone using an analytical Apollo C18 column (250 mm × 4.6 mm, 5 μm, Grace Davison Discovery Sciences) with the same solvents and gradient as above with a flow rate of 1 ml/min, were combined and the solvent removed under reduced pressure yielding a white crystalline solid. Pure 4-methyl-2-oxobutyrolactone was dissolved in water and an equimolar amount of NaOH (1 M) was added leading to a final concentration of 50 mM (Dagley and Gibson, 1965). After incubation overnight at 20 °C, the pH of the solution was adjusted to 7.0 using 3.5% HCl. HKV was stored at −21 °C until required.

2.2. Expression and purification of DmpFG

DmpFG was expressed and purified as described by Lei et al. (2008) with some modifications. *Escherichia coli* C41 (DE3) cells were grown at 37 °C with the expression of DmpFG induced at OD_{600} 0.6–0.8 with 1 mM isopropyl β-D-1-thiogalactopyranoside and then incubated for a further 3 h. All steps in the purification were performed at 4 °C. The cell pellet was resuspended in 50 mM K^+/Na^+ phosphate buffer (pH 7.5) with 1 mM DTT (PD buffer). The cells were lysed by sonication and centrifuged for 40 min at 17,000 × *g*. The supernatant was applied to a DEAE fast flow anion exchange column (5 ml) (GE Healthcare) pre-equilibrated with PD buffer, and the protein eluted with PD buffer containing 275 mM NaCl. Fractions were assayed for dehydrogenase activity (Section 2.4) and active fractions combined. Ammonium sulphate was added to the combined fractions to 15% saturation and the precipitate removed by centrifugation at 4000 × *g* prior to filtration. The resulting filtrate was applied to a phenyl-sepharose fast-flow high performance hydrophobic affinity column (20 ml) (GE Healthcare) pre-equilibrated with PD buffer containing 15% saturated

ammonium sulphate. DmpFG was eluted from the column with a linear gradient from 15–0% ammonium sulphate. Fractions containing DmpFG to a suitable level of purity, as assessed by SDS polyacrylamide gel electrophoresis, were combined and dialysed into K^+/Na^+ phosphate buffer (pH 8.0) with 1 mM DTT. DmpFG was concentrated to 3 mg/ml using a Vivaspin 20 10 kDa cut-off Millipore centricon (GE Healthcare), as determined by Bradford analysis using BSA as a standard (Bradford, 1976), and stored at −80 °C.

2.3. Steady state forward DmpFG assays

Standard assays used 50 mM K^+/Na^+ phosphate buffer (pH 8.0) in a total volume of 1 ml. Saturating concentrations of HKV, NAD^+ and CoA (Sigma–Aldrich) were 2 mM, 1 mM and 0.6 mM respectively. The aldolase and dehydrogenase reaction were monitored using spectrophotometry at 340 nm by the conversion of NAD^+ to NADH in DmpF. The assay mixtures were pre-equilibrated in a water bath for 10 min at 30 °C, the background absorbance measured for 2 min prior to the addition of protein (30 μg/ml) and the reaction was monitored for a further 2 min. To obtain the HKV dependence of the aldolase, the HKV concentration was varied from 0.1 K_m to 10 K_m while NAD^+ and CoA were maintained at saturating concentrations. The data were fitted by non-linear least-squares regression using the program PRISM to Eq. (1) where A is the concentration of HKV:

$$v = \frac{V_{max}A}{K_m + A} \quad (1)$$

To obtain the NAD^+ dependence of the DmpF-catalyzed reaction, the NAD^+ concentration was varied from 0.1 K_m to 60 K_m while HKV and CoA were maintained at saturating concentrations. The data were fitted by non-linear least-squares regression using the program PRISM with Eq. (2) where A is the concentration of NAD^+, and K_m and K_i are the Michaelis constant and the substrate inhibition constant of NAD^+ respectively:

$$v = \frac{V_{max}A}{(A + K_m)(1 + A/K_i)} \quad (2)$$

Finally, to obtain the CoA dependence of the dehydrogenase DmpF, CoA was varied from 0.1 K_m to 10 K_m while HKV and NAD^+ were maintained at saturating concentrations. The data were fitted by non-linear least-squares regression using the program PRISM to Eq. (1), where A is the concentration of CoA.

2.4. Forward DmpF dehydrogenase assay

Standard assays were performed as above using saturating concentrations of CoA and NAD^+, but rather than HKV, exogenous acetaldehyde (Sigma–Aldrich) was varied from 0.001 K_m to 4 K_m. The data were fitted by non-linear least-squares regression using the program PRISM to Eq. (1), where A is the concentration of acetaldehyde. Prior to use, 1 ml aliquots of acetaldehyde solutions (diluted from the stock solution to approximately 0.025 mM) were assayed in triplicate using alcohol dehydrogenase from *Saccharomyces cerevisiae* (0. 5 μg/ml) (Sigma–Aldrich) with 0.1 mM NADH in 50 mM K^+/Na^+ phosphate (pH 8.0). The reaction was monitored directly by following the loss of NADH at 340 nm until no further change in absorbance was observed, indicating that all of the acetaldehyde in the solution had been consumed.

2.5. Reverse DmpF dehydrogenase assay

The reverse DmpF dehydrogenase assays were carried out using four NADH concentrations: 0.2, 0.3, 0.5 and 0.8 mM. At 0.2 and 0.3 mM NADH, 1 ml cuvettes with a path length of 1 cm were used. At 0.5 and 0.8 mM NADH, a 100 μl quartz cuvette with a path length of 0.3 cm was utilized. The acetyl CoA (Sigma–Aldrich) concentration was varied from 0.1 K_m to 50 K_m for each data set. The pyruvate (Sigma–Aldrich) concentration was maintained at 10 mM and 50 mM K^+/Na^+ phosphate (pH 8.0) was used. The dehydrogenase activity was monitored directly by measuring the loss of NADH using spectrophotometry at 340 nm. The assay mixtures were pre-equilibrated in a water bath for 10 min at 30 °C, the background absorbance measured for 2 min prior to the addition of protein (0.1 mg/ml) and the reaction monitored for a further 3–5 min. The data were globally fitted by non-linear least-squares regression in PRISM using Eq. (3), which describes a ping-pong reaction (Cleland, 1963a,b) exhibiting substrate inhibition, where A is the concentration of acetyl CoA, B is the concentration of NADH, K_a and K_b are the Michaelis constants for acetyl CoA and NADH respectively and K_{ia} is the substrate inhibition constant for acetyl CoA (Cleland, 1979):

$$v = \frac{V_{max}AB}{K_bA(1 + A/K_{ia}) + K_aB + AB} \quad (3)$$

2.6. Temperature dependence of the aldolase DmpG and the dehydrogenase DmpF

Each assay was performed in duplicate at 20, 25, 30 and 35 °C. Prior to the addition of the protein, solutions were equilibrated for 10 min at the appropriate temperature. For the dehydrogenase DmpF assays, 1 ml solutions contained 100 mM acetaldehyde, with saturating concentrations of CoA and NAD^+ in 50 mM K^+/Na^+ phosphate (pH 8.0). The dehydrogenase activity was followed directly by monitoring the formation of NADH at 340 nm. After equilibration, the background absorbance was measured for 2 min prior to the addition of protein (30 μg/ml) and data collected for 2–3 min. For the aldolase DmpG assays, the activity was monitored at 340 nm using a lactate dehydrogenase (LDH) coupled assay, where the amount of pyruvate formed from the consumption of HKV by DmpG was measured by conversion of NADH to NAD^+ in LDH. 1 ml solutions contained a saturating concentration of HKV with NADH at a concentration of 0.1 mM in 50 mM K^+/Na^+ phosphate (pH 8.0), all other conditions were maintained as described above. Finally, to obtain the temperature dependence of the full DmpFG forward reaction HKV, NAD^+ and CoA concentrations were saturating using 50 mM K^+/Na^+ phosphate (pH 8.0) in a total volume of 1 ml. This reaction was followed via the conversion of NAD^+ to NADH by the dehydrogenase DmpF. An Arrhenius plot was obtained for each dataset and the gradient (=$-E_a/R$) was obtained by linear regression using the program PRISM.

2.7. Forward channeling assay

Each assay was performed in triplicate at 20, 25, 30 and 35 °C. Standard assays contained 0.6 mM CoA, 0.6 mM NAD^+ and 0.20 mM HKV with 50 mM K^+/Na^+ phosphate (pH 8.0) in a total volume of 1 ml. Assay solutions were equilibrated in a water bath for 10 min at the appropriate temperature and the background absorbance at 340 nm recorded for 2 min prior to the addition of DmpFG (30 μg/ml). The reaction was then monitored until no further change in absorbance was observed. The total change in absorbance measured was equivalent to the amount of HKV consumed in the DmpG reaction which successfully formed acetyl CoA by DmpF (1 in Eq. (4) below). The sample was then placed on ice and the enzyme removed by filtration using a 10 kDa cut-off membrane (Millipore) at 1800 × *g*. A portion of the filtrate (800 μl) was combined with additional buffer and the volume adjusted to give a final volume of 1 ml. The background absorbance was determined as described above and alcohol dehydrogenase from *S. cerevisiae* (0. 5 μg/ml) added to catalyze the conversion of acetaldehyde, released from the previous reaction, to ethanol, with concomitant oxidation of

Table 1
Kinetic parameters for the DmpFG reaction.

Varied substrate	V_{max} (U mg^{-1})	K_m (mM)	K_i (mM)	k_{cat} (s^{-1})	k_{cat}/K_m ($\times 10^3$ M^{-1} s^{-1})
HKV	2.30 ± 0.039	0.18 ± 0.011	NA	26.8	149.1
NAD^+	2.17 ± 0.088	0.16 ± 0.016	6.19 ± 0.74	25.3	158.2
CoA	2.34 ± 0.068	0.076 ± 0.010	NA	27.3	359.2

Table 2
Kinetic parameters for the dehydrogenase DmpF reaction.

Varied substrate	V_{max} (U mg^{-1})	K_m (mM)	K_i (mM)	k_{cat} (s^{-1})	k_{cat}/K_m ($\times 10^3$ M^{-1} s^{-1})
Acetaldehyde[a]	10.0 ± 0.224	23.7 ± 1.48	NA	116.7	4.92

[a] Exogenous acetaldehyde was used to determine these values.

NADH. The total change in absorbance, due to NADH oxidation, is proportional to the amount of acetaldehyde that has escaped from the channel prior to conversion to acetyl CoA by DmpF (2 in Eq. (4) below) as it is assumed that acetaldehyde released into the bulk media will not undergo reaction with DmpF. Given the high K_m value obtained for exogenous acetaldehyde in the DmpF reaction this seems reasonable. The channeling efficiency (CE) of DmpFG was calculated using Eq. (4) as shown below:

$$\mathrm{CE}(\%) = \frac{(1)}{(1)+(2)} \times 100 \quad (4)$$

In order to ensure that NADH was not limiting, the same process was repeated as above but supplementary NADH (0.1 mM) was added prior to the addition of alcohol dehydrogenase. Finally, additional acetaldehyde was added to the reaction mixture after the initial end point of the reaction had been reached, allowing the reaction to continue provided no other substrate was limiting.

3. Results and discussion

3.1. Kinetic characteristics of DmpFG

BphI-BphJ, an orthologue of DmpFG from *Burkholderia xenovorans* LB400, where BphI and BphJ have 56 and 55% sequence identity with DmpG and DmpF respectively, has been kinetically characterized as wild type and as a series of mutants (Baker et al., 2009, 2011, 2012a,b; Baker and Seah, 2011; Carere et al., 2011; Wang et al., 2010; Wang and Seah, 2005). More recently, the orthologous enzyme complexes MhpEF, from both *E. coli* (EcMhpEF) and *Thermomonospora curvata* (TcMhpEF) were investigated (Fischer et al., 2013), where MhpE and MhpF have 80 and 76% sequence identity with DmpG and DmpF respectively (Baker et al., 2012b). This study focused on the activity of the dehydrogenase MhpF both in complex with MhpE and as a monomer. In each case, exogenous acetaldehyde was utilized, such that the reaction by the aldolase, MhpE, was not studied. In the current kinetic study of DmpFG two main objectives were investigated: (1) to characterize the kinetics of the dehydrogenase, DmpF, individually and in the context of the complete DmpFG reaction and (2) to investigate the substrate channeling process within DmpFG.

The overall DmpFG reaction pathway was characterized for the forward reaction, beginning with HKV under saturating concentrations of CoA and NAD^+. This allowed acetaldehyde to be transported directly from the aldolase to the dehydrogenase through the buried molecular channel as would occur under the physiological conditions of the enzyme. K_m and k_{cat} values were obtained for each of the substrates involved in the forward reaction of DmpFG. It was found that HKV had a K_m of 0.18 mM and a k_{cat} of 27.6 s^{-1} (Fig. 2A and Table 1). When analysing the forward reaction of the dehydrogenase, K_m values of 0.16 mM and 0.076 mM were obtained for NAD^+ and CoA respectively (Fig. 2 B and C and Table 1) and high concentrations of NAD^+ inhibited the dehydrogenase reaction with a K_i of 6.19 mM. When this same reaction was studied in isolation from the aldolase DmpG, using exogenous acetaldehyde rather than HKV, we obtained a non-physiological K_m of 23.7 mM for acetaldehyde indicating a low substrate affinity (Fig. 3 and Table 2). However, in spite of the high K_m, the k_{cat} obtained for DmpF was approximately four times higher (120 s^{-1}) than that observed for the dehydrogenase reaction when the acetaldehyde was channeled directly from the aldolase DmpG, indicating that under the current experimental conditions the aldolase limits the rate of the overall DmpFG reaction.

Of the orthologues investigated to date, EcMhpEF has the highest sequence identity with DmpFG (Baker et al., 2012b; Fischer et al., 2013). Monomeric EcMhpF had K_m values of 0.25 mM and 0.09 mM for NAD^+ and CoA respectively (Fischer et al., 2013) which are in good agreement with the values obtained for DmpF. Similarly to DmpF, MhpF was also inhibited by high concentrations of NAD^+ (Fischer et al., 2013). In contrast, a K_m of 1.45 mM was obtained for NAD^+ in the complex EcMhpEF, approximately nine times higher than that observed for DmpF. The K_m values obtained for DmpF were approximately five and two fold higher than the values obtained for NAD^+ and CoA respectively, in BphJ (Baker et al., 2012a). This difference may be explained by the fact that Baker et al. (2012a) obtained these values using exogenous acetaldehyde excluding the aldolase BphI from the reaction, however, as the investigations on MhpEF also utilized exogenous acetaldehyde the observed differences in K_m may demonstrate differences in the enzymes in question rather than the experimental conditions. Of interest, the K_m value obtained for exogenous acetaldehyde in DmpF was nearly identical to that obtained for BphJ (23.6 mM). These high values indicate a low substrate affinity and demonstrate the need for direct delivery of the aldehyde intermediate from the aldolase to the dehydrogenase via the buried molecular channel.

Further to this investigation we observed the reverse (non-physiological) reaction of the dehydrogenase DmpF using NADH and acetyl CoA as shown in Fig. 4 as it allowed the analysis of a two reactant rather than a three reactant system. Initially, an attempt

Table 3
Kinetic parameters for the DmpFG reverse reaction.

Varied substrate	V_{max} (U mg^{-1})	K_m (mM)	K_i (mM)	k_{cat} (s^{-1})	k_{cat}/K_m ($\times 10^3$ M^{-1} s^{-1})
NADH	5.25 ± 0.158	0.057 ± 0.013	NA	61.3	1075
Acetyl CoA	5.25 ± 0.158	0.18 ± 0.012	1.36 ± 0.32	61.3	340.3

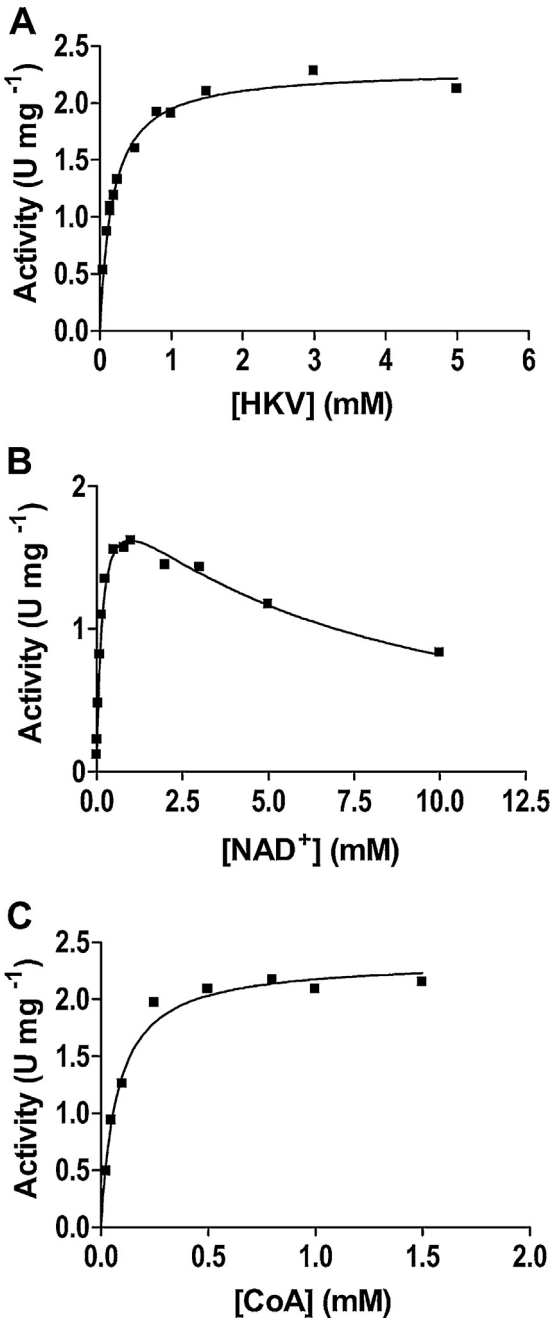

Fig. 2. Plots of the steady-state activity in the forward reaction of DmpFG, the solid lines represent non-linear regression fits of the data to Eq. (1) – (A) and (C) or Eq. (2) – (B). (A) At saturating concentrations of CoA and NAD^+, while the HKV concentration was varied from 0.1 K_m to 20 K_m. (B) At saturating concentrations of HKV and CoA, while the NAD^+ concentration was varied from 0.1 K_m to 60 K_m. (C) At saturating concentrations of HKV and NAD^+, while the CoA concentration was varied from 0.1 K_m to 10 K_m.

was made to fit that data to an equation describing a sequential reaction with substrate inhibition, however, this resulted in an estimate of K_{ia} that had a negative value. Ultimately, the data was successfully fitted using Eq. (3), supporting the conclusion that DmpF undergoes a two substrate ping-pong mechanism with the formation of an acyl-intermediate, as initially hypothesized by Manjasetty et al. (2003). These results complement previous data obtained for DmpF (Lei et al., 2008) and for MhpF (Fischer et al., 2013) which supported the use of a ping-pong mechanism. Indeed, these results suggest that DmpF shares characteristics with other CoA-linked ALDHs (Rudolph et al., 1968; Shone and

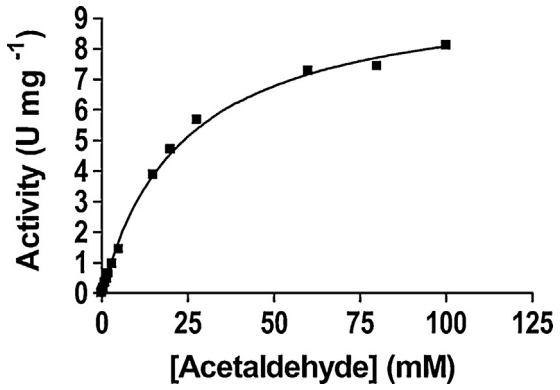

Fig. 3. Plot of the steady-state activity for the reaction of the dehydrogenase DmpF reaction, the solid line represents a non-linear regression fit of the data to Eq. (1). CoA and NAD^+ were saturating while the concentration of exogenous acetaldehyde was varied from 0.001 K_m to 4 K_m.

Fromm, 1981; Smith and Kaplan, 1980; Yan and Chen, 1990) and with the CoA dependent succinate–semialdehyde dehydrogenase from *C. kluyveri* (Sohling and Gottschalk, 1993) which also exhibit ping-pong kinetics. In this study of DmpF, the specific Michaelis constants obtained for NADH and acetyl CoA were 0.058 mM and 0.18 mM (Table 3) respectively.

Of interest, high concentrations of acetyl CoA inhibited DmpF with a K_i of 1.36 mM. Given the ping-pong mechanism catalyzed by the dehydrogenase, the observed substrate inhibition indicates acetyl CoA is competing with NADH to bind to $E_1E'_2$ (Fig. 5) and NAD^+ probably competes with CoA for $E_1E'_2$. Hence we see inhibition at high acetyl CoA in the reverse reaction and at high NAD^+ in the forward reaction. The acetyl CoA inhibition reported here appears to be unique in the literature for this class of dehydrogenase. While the formation of an enzyme-CoA dead end complex has been proposed for other CoA-linked dehydrogenases (Smith and Kaplan, 1980) no CoA inhibition was observed for DmpF. The mechanism suggests that this inhibition in the forward reaction would require CoA to compete with NAD^+ for binding to E_1E_2. AALD and NADH would have to compete with acetyl CoA for binding to E_1E_2 in the reverse reaction. Since the mechanism is designed to be strictly ordered, this may not occur so readily.

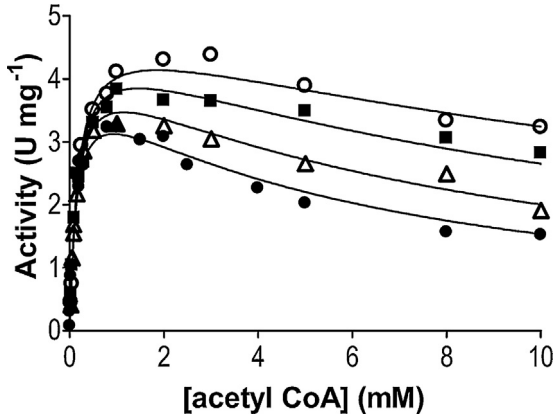

Fig. 4. Plots of the steady-state activity for the reverse reaction of DmpFG, the solid lines represent a global non-linear regression fit of the data to Eq. (3). The NADH concentration was kept constant for each curve with values of 0.2 mM (●), 0.3 mM (△), 0.5 mM (■) and 0.8 mM (○), while the acetyl CoA concentration was varied from 0.1 K_m to 50 K_m. The pyruvate concentration for all assays was fixed at 10 mM.

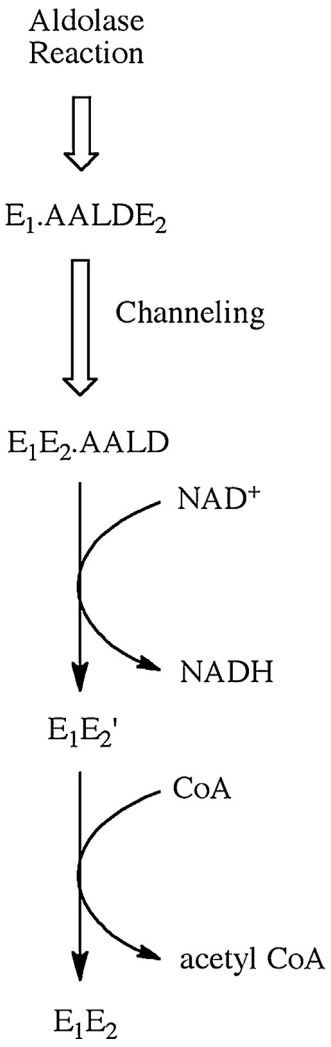

Fig. 5. The reaction pathway of DmpF, where E_1 is DmpG, E_2 is DmpF and E'_2 is the thioacylated form of DmpF. The intermediate states of the enzyme complex are shown with the substrates: NAD^+ and CoA, the intermediate acetaldehyde (AALD) and with the products of the enzyme reaction: NADH and acetyl CoA.

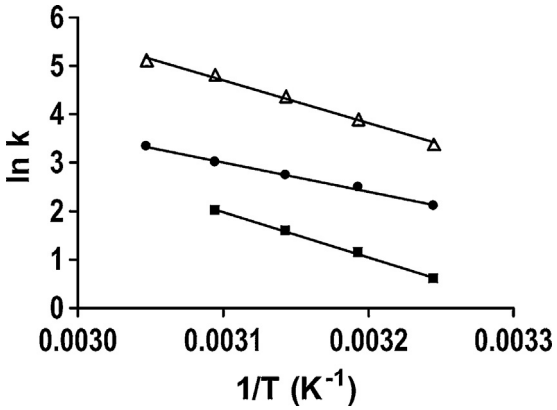

Fig. 6. Arrhenius plots depict the temperature dependence of the rate constants of the aldolase, DmpG (■), the dehydrogenase, DmpF (Δ) and the full enzyme system DmpFG (●). The solid lines represent fits of the data using linear regression analysis.

3.2. Activation parameters for the aldolase, the dehydrogenase and the DmpFG reactions

The thermodynamic activation parameters of the aldolase DmpG, the dehydrogenase DmpF and for the whole enzyme complex were determined using Arrhenius plots (Fig. 6) where the slope equals $-E_a/R$ (where E_a is the activation energy and R is the universal gas constant). E_as of 18.5 ± 0.6, 17.7 ± 0.8 and 12.0 ± 0.5 kcal/mol were obtained for the aldolase, the dehydrogenase and the DmpFG complex respectively, indicating that the E_a required for the linked reaction in DmpFG is significantly lower than that required for each enzyme individually. This appears to be due to a favorable reduction in the enthalpy of activation ($\Delta H^{\ddagger}$) (Table 4) indicating the possibility of allosteric changes to the structure of the protein, with the formation of new hydrogen bonds or hydrophobic and ionic interactions in the transition state of the rate-limiting step (Truong et al., 2011). The change in $\Delta H^{\ddagger}$ is coupled with an unfavorable reduction in the entropy ($T\Delta S^{\ddagger}$), implying that the transition state of the rate-limiting step of the reaction catalyzed by the DmpFG complex is more ordered when both enzymes are participating in the reaction pathway. This unfavorable change in $T\Delta S^{\ddagger}$ resulted in a higher $\Delta G^{\ddagger}$ for the overall DmpFG reaction, when compared to the individual reaction of the dehydrogenase. This is in agreement with our previous finding that the k_{cat} of the individual dehydrogenase reaction was significantly higher than that obtained for the DmpFG reaction.

3.3. Allosteric activation in DmpFG

The $\Delta G^{\ddagger}$ for the aldolase reaction is greater than that of the overall DmpFG reaction which may indicate that the release of acetaldehyde, which does not occur in the DmpFG reaction, is rate-limiting. Another possibility, is that when both the DmpG and DmpF reactions are occurring in sequence, the structure of the aldolase is allosterically modified, enhancing the rate of the aldolase reaction. This possibility is supported by results obtained for DmpFG, where the aldolase activity was enhanced by the presence of both NAD^+ and NADH (Powlowski et al., 1993) and for BphI–BphJ where 5-fold activation was noted for BphI in the presence of NADH (Baker et al., 2009, 2012a; Carere et al., 2011). While Manjasetty et al. (2003) suggested that this activation could be a factor of the channel opening in the presence of NAD^+, site directed mutagenesis studies of BphI–BphJ indicated that this change in reaction rate was not due to the channeling event but was most likely a factor of changes to the proteins structure (Baker et al., 2012a). Baker et al. (2009) found that the activation of BphI by NADH was not due to an increase in the pyruvate proton transfer rate, implying that the change triggering this alteration in aldolase activity must occur prior to this step, possibly in the base-catalyzed abstraction of the initial substrates hydroxyl group (Baker et al., 2009).

To date, the structural change, or changes, leading to increased activity in the aldolase DmpG have not been determined. While the structure of DmpFG was obtained in both the apo and holoenzyme form no significant difference was noted in the active site of the aldolase regardless of whether or not NAD^+ was bound to

Table 4
Thermodynamic activation parameters.

Aldolase					
Temperature (K)	308.15	313.15	318.15	323.15	328.15
$\Delta H^{\ddagger}$ (kcal/mol)	17.92	17.91	17.90	17.89	NA
$T\Delta S^{\ddagger}$ (kcal/mol)	0.232	0.264	0.244	0.217	NA
$\Delta G^{\ddagger}$ (kcal/mol)	17.69	17.65	17.66	17.67	NA
Dehydrogenase					
$\Delta H^{\ddagger}$ (kcal/mol)	17.04	17.03	17.02	17.01	17.00
$T\Delta S^{\ddagger}$ (kcal/mol)	1.05	1.09	1.12	1.13	1.06
$\Delta G^{\ddagger}$ (kcal/mol)	15.99	15.94	15.90	15.88	15.94
DmpFG					
$\Delta H^{\ddagger}$ (kcal/mol)	11.36	11.35	11.34	11.33	11.32
$T\Delta S^{\ddagger}$ (kcal/mol)	−5.41	−5.46	−5.59	−5.70	−5.77
$\Delta G^{\ddagger}$ (kcal/mol)	16.77	16.81	16.93	17.03	17.09

Table 5
Substrate channeling efficiencies for acetaldehyde in DmpFG.

Temperature (°C)	Without added NADH (%)	+ 0.1 mM NADH (%)
20	91 ± 4	87 ± 7
25	95 ± 1	89 ± 3
30	90 ± 4	90 ± 1
35	94 ± 1	92 ± 3

DmpF (Manjasetty et al., 2003). However, in each case, a pyruvate analog (oxalate) was bound to DmpG. Given the findings of Baker et al. (2009), regarding the point of aldolase activation during the reaction sequence, this suggests that the observed structural arrangement may not represent the activated form of the enzyme. Allosteric interactions have been reported and investigated for other closely linked channeling enzymes including carbamoyl phosphate synthetase (Miles and Raushel, 2000; Thoden et al., 2004) and tryptophan synthase (Anderson et al., 1991; Brzović et al., 1992). Based on the cumulative results obtained to date for DmpFG and its orthologues it would be interesting to gain further structural insight into how the allosteric activation of the aldolase occurs when the reaction is occurring within the dehydrogenase.

3.4. Substrate channeling in DmpFG

While substrate channeling has never been shown to occur experimentally within the enzyme DmpFG, this process has been extensively investigated in the orthologue BphI–BphJ showing that acetaldehyde and a series of longer chained aldehydes can be efficiently channeled (Baker et al., 2009, 2012a; Carere et al., 2011; Wang et al., 2010). Channeling has also been demonstrated in the orthologous enzymes TTHB246–TTHB247 from *Thermus thermophilus* and in chimeric complexes of BphI–TTHB247 and TTHB246–BphJ (Baker et al., 2012b). In the case of DmpFG we obtained the CE of acetaldehyde using a different method, however our value of 95% at 25 °C (Table 5), is identical to the value obtained for BphI–BphJ (Carere et al., 2011) and similar to the value obtained for TTHB246–TTHB247 (94%) (Baker et al., 2012b).

MD simulations had indicated that acetaldehyde was able to escape the channel through pathways that opened to bulk media in the matrix of the protein (Smith et al., 2012). In this case we wanted to investigate the effect of temperature on the channeling process as it was hypothesized that, as the flexibility of the protein increases with temperature, so would the possibility of the acetaldehyde escaping from the channel prematurely. However, no temperature dependence was found as DmpFG had a consistently high CE for acetaldehyde with means of 93 ± 3% and 90 ± 4% in the absence, and presence of additional NADH respectively, indicating that approximately 10% of the acetaldehyde escapes the channel prior to reaching the dehydrogenase active site in each case.

4. Concluding remarks

In conclusion, we have shown that DmpF catalyses a ping-pong mechanism with inhibition by acetyl CoA in the reverse reaction and NAD^+ in the forward reaction. It was noted, that the k_{cat} obtained for the isolated dehydrogenase reaction, was significantly higher than that which was obtained for the full DmpFG reaction. We subsequently found that the dehydrogenase reaction had the lowest $\Delta G^{\ddagger}$ when compared to both the isolated aldolase reaction and the full DmpFG reaction, supporting the high k_{cat} value. Of interest, the full DmpFG reaction occurs with a large, unfavorable change in $\Delta S^{\ddagger}T$. This was not observed for either of the individual enzyme reactions and, as such, it appears to support the use of allosteric structural modifications between the two enzymes, enhancing the rate of the aldolase reaction. Finally, we have shown that DmpFG channels acetaldehyde with a high CE in the same range as that which has been observed for other aldolase–dehydrogenase complexes (Baker et al., 2012b; Carere et al., 2011).

Acknowledgements

KAS and GRF acknowledge funding from the Australian Research Council (FT100100291 and FT110100304 respectively). NES acknowledges support through an Australian Postgraduate Award and a Jean Rogerson Scholarship.

References

Ahvazi B, Coulombe R, Delarge M, Vedadi M, Zhang L, Meighen E, et al. Crystal structure of the NADP+-dependent aldehyde dehydrogenase from *Vibrio harveyi*: structural implications for cofactor specificity and affinity. Biochemical Journal 2000;349(Pt. 3):853–61.
Anderson KS, Miles EW, Johnson KA. Serine modulates substrate channeling in tryptophan synthase. A novel intersubunit triggering mechanism. Journal of Biological Chemistry 1991;266:8020–33.
Baker P, Carere J, Seah SYK. Probing the molecular basis of substrate specificity, stereospecificity, and catalysis in the class II pyruvate aldolase, BphI. Biochemistry 2011;50:3559–69.
Baker P, Carere J, Seah SYK. Substrate specificity, substrate channeling, and allostery in BphJ: an acylating aldehyde dehydrogenase associated with the pyruvate aldolase BphI. Biochemistry 2012a;51:4558–67.
Baker P, Hillis C, Carere J, Seah SYK. Protein–protein interactions and substrate channeling in orthologous and chimeric aldolase–dehydrogenase complexes. Biochemistry 2012b;51:1942–52.
Baker P, Pan D, Carere J, Rossi A, Wang W, Seah SYK. Characterization of an aldolase–dehydrogenase complex that exhibits substrate channeling in the polychlorinated biphenyls degradation pathway. Biochemistry 2009;48:6551–8.
Baker P, Seah SYK. Rational design of stereoselectivity in the Class II pyruvate aldolase BphI. Journal of the American Chemical Society 2011;134:507–13.
Brecher AS, Hellman K, Basista MH. A perspective on acetaldehyde concentrations and toxicity in man and animals. Alcohol 1997;14:493–6.
Brzović PS, Ngo K, Dunn MF. Allosteric interactions coordinate catalytic activity between successive metabolic enzymes in the tryptophan synthase bienzyme complex. Biochemistry 1992;31:3831–9.
Carere J, Baker P, Seah SYK. Investigating the molecular determinants for substrate channeling in BphI–BphJ, an aldolase–dehydrogenase complex from the Polychlorinated biphenyls degradation pathway. Biochemistry 2011;50:8407–16.
Chaudhuri BN, Lange SC, Myers RS, Chittur SV, Davisson VJ, Smith JL. Crystal structure of imidazole glycerol phosphate synthase: a tunnel through a (beta/alpha)8 barrel joins two active sites. Structure 2001;9:987–97.
Cleland W. The kinetics of enzyme catalysed reactions with two or more substrates or products. II. Inhibition: nomenclature and theory. Biochimica et Biophysica Acta 1963b;67:173–87.
Cleland WW. The kinetics of enzyme catalysed reactions with two or more substrates or products. I. Nomenclature and rate equations. Biochimica et Biophysica Acta 1963a;67:104–37.
Cleland WW. Substrate inhibition. Methods in Enzymology 1979;63:500–13.
Cobessi D, Tete-Favier F, Marchal S, Azza S, Branlant G, Aubry A. Apo and holo crystal structures of an NADP-dependent aldehyde dehydrogenase from *Streptococcus mutans*. Journal of Molecular Biology 1999;290:161–73.
Cobessi D, Tete-Favier F, Marchal S, Branlant G, Aubry A. Structural and biochemical investigations of the catalytic mechanism of an NADP-dependent aldehyde dehydrogenase from *Streptococcus mutans*. Journal of Molecular Biology 2000;300:141–52.
D'Ambrosio K, Pailot A, Talfournier F, Didierjean C, Benedetti E, Aubry A, et al. The first crystal structure of a thioacylenzyme intermediate in the ALDH family: new coenzyme conformation and relevance to catalysis. Biochemistry 2006;45:2978–86.
Dagley S, Gibson D. The bacterial degradation of catechol. Biochemical Journal 1965;95:466–74.
Darnault C, Volbeda A, Kim EJ, Legrand P, Vernede X, Lindahl PA, et al. Ni–Zn–[Fe4–S4] and Ni–Ni–[Fe4–S4] clusters in closed and open subunits of acetyl-CoA synthase/carbon monoxide dehydrogenase. Natural Structural Biology 2003;10:271–9.
Doukov TI, Iverson TM, Seravalli J, Ragsdale SW, Drennan CL. A Ni–Fe–Cu center in a bifunctional carbon monoxide dehydrogenase/acetyl–CoA synthase. Science 2002;298:567–72.
Drennan CL, Heo J, Sintchak MD, Schreiter E, Ludden PW. Life on carbon monoxide: X-ray structure of *Rhodospirillum rubrum* Ni–Fe–S carbon monoxide dehydrogenase. Proceedings of the National Academy of Sciences of the United States of America 2001;98:11973–8.
Dubourg H, Stines-Chaumeil C, Didierjean C, Talfournier F, Rahuel-Clermont S, Branlant G, et al. Expression, purification, crystallization and preliminary X-ray diffraction data of methylmalonate–semialdehyde dehydrogenase from

Bacillus subtilis. Acta Crystallographica Section D: Biological Crystallography 2004;60:1435–7.
Farres J, Wang TT, Cunningham SJ, Weiner H. Investigation of the active site cysteine residue of rat liver mitochondrial aldehyde dehydrogenase by site-directed mutagenesis. Biochemistry 1995;34:2592–8.
Feldman RI, Weiner H. Horse liver aldehyde dehydrogenase. II. Kinetics and mechanistic implications of the dehydrogenase and esterase activity. Journal of Biological Chemistry 1972;247:267–72.
Fischer B, Boutserin S, Mazon H, Collin S, Branlant G, Gruez A. Catalytic properties of a bacterial acylating acetaldehyde dehydrogenase: evidence for several oligomeric states and coenzyme A activation upon binding. Chemico-Biological Interactions 2013.
Hadfield A, Kryger G, Ouyang J, Petsko GA, Ringe D, Viola R. Structure of aspartate-beta-semialdehyde dehydrogenase from *Escherichia coli*, a key enzyme in the aspartate family of amino acid biosynthesis. Journal of Molecular Biology 1999;289:991–1002.
Huang X, Holden HM, Raushel FM. Channeling of substrates and intermediates in enzyme-catalyzed reactions. Annual Review of Biochemistry 2001;70:149–80.
Hyde CC, Ahmed SA, Padlan EA, Miles EW, Davies DR. Three-dimensional structure of the tryptophan synthase alpha 2 beta 2 multienzyme complex from *Salmonella typhimurium*. Journal of Biological Chemistry 1988;263:17857–71.
Kim JH, Krahn JM, Tomchick DR, Smith JL, Zalkin H. Structure and function of the glutamine phosphoribosylpyrophosphate amidotransferase glutamine site and communication with the phosphoribosylpyrophosphate site. Journal of Biological Chemistry 1996;271:15549–57.
Knighton DR, Kan CC, Howland E, Janson CA, Hostomska Z, Welsh KM, et al. Structure of and kinetic channeling in bifunctional dihydrofolate reductase–thymidylate synthase. Natural Structural Biology 1994;1:186–94.
Krahn JM, Kim JH, Burns MR, Parry RJ, Zalkin H, Smith JL. Coupled formation of an amidotransferase interdomain ammonia channel and a phosphoribosyltransferase active site. Biochemistry 1997;36:11061–8.
Larsen TM, Boehlein SK, Schuster SM, Richards NG, Thoden JB, Holden HM, et al. Three-dimensional structure of *Escherichia coli* asparagine synthetase B: a short journey from substrate to product. Biochemistry 1999;38:16146–57.
Lei Y, Pawelek PD, Powlowski J. A shared binding site for NAD^+ and coenzyme A in an acetaldehyde dehydrogenase involved in bacterial degradation of aromatic compounds. Biochemistry 2008;47:6870–82.
Liu ZJ, Sun YJ, Rose J, Chung YJ, Hsiao CD, Chang WR, et al. The first structure of an aldehyde dehydrogenase reveals novel interactions between NAD and the Rossmann fold. Natural Structural Biology 1997;4:317–26.
Manjasetty BA, Powlowski J, Vrielink A. Crystal structure of a bifunctional aldolase–dehydrogenase: sequestering a reactive and volatile intermediate. Proceedings of the National Academy of Sciences of the United States of America 2003;100:6992–7.
Milani M, Pesce A, Bolognesi M, Bocedi A, Ascenzi P. Substrate channeling. Biochemistry and Molecular Biology Education 2003;31:228–33.
Miles BW, Raushel FM. Synchronization of the three reaction centers within carbamoyl phosphate synthetase. Biochemistry 2000;39:5051–6.
Miles EW, Rhee S, Davies DR. The molecular basis of substrate channeling. Journal of Biological Chemistry 1999;274:12193–6.
Muchmore CR, Krahn JM, Kim JH, Zalkin H, Smith JL. Crystal structure of glutamine phosphoribosylpyrophosphate amidotransferase from *Escherichia coli*. Protein Science 1998;7:39–51.
Powlowski J, Sahlman L, Shingler V. Purification and properties of the physically associated meta-cleavage pathway enzymes 4-hydroxy-2-ketovalerate aldolase and aldehyde dehydrogenase (acylating) from Pseudomonas sp. strain CF600. Journal of Bacteriology 1993;175:377–85.
Racker E, Krimsky I. The mechanism of oxidation of aldehydes by glyceralde-hyde-3-phosphate dehydrogenase. Journal of Biological Chemistry 1952;198:731–43.
Rossi A, Schinz H. Alcuni a-cheto-g-lattoni con sostituenti alchilici in posizione g. Helvetica Chimica Acta 1948;31:473–92.
Rudolph FB, Purich DL, Coenzyme Fromm HK. A-linked aldehyde dehydrogenase from *Escherichia coli*. I. Partial purification, properties and kinetic studies of the enzyme. Journal of Biological Chemistry 1968;243:5539–45.
Segal HL, Boyer PD. The role of sulfhydryl groups in the activity of D-glyceraldehyde 3-phosphate dehydrogenase. Journal of Biological Chemistry 1953;204:265–81.
Shingler V, Powlowski J, Marklund U. Nucleotide sequence and functional analysis of the complete phenol/3,4-dimethylphenol catabolic pathway of *Pseudomonas* sp. strain CF600. Journal of Bacteriology 1992;174:711–24.
Shone CC, Fromm HJ. Steady-state and pre-steady-state kinetics of Coenzyme A Linked Aldehyde dehydrogenase from *Escherichia coli*. Biochemistry 1981;20:7494–501.
Smith JL, Zaluzec EJ, Wery JP, Niu L, Switzer RL, Zalkin H, et al. Structure of the allosteric regulatory enzyme of purine biosynthesis. Science 1994;264:1427–33.
Smith LT, Kaplan NO. Purification, properties, and kinetic mechanism of Coenzyme A-Linked aldehyde dehydrogenase from *Clostridium kluyveri*. Archives of Biochemistry and Biophysics 1980;203:663–75.
Smith NE, Vrielink A, Attwood PV, Corry B. Biological channeling of a reactive intermediate in the bifunctional enzyme DmpFG. Biophysical Journal 2012;102:868–77.
Sohling B, Gottschalk G. Purification and characterization of a coenzyme-A-dependent succinate–semialdehyde dehydrogenase from *Clostridium kluyveri*. European Journal of Biochemistry 1993;212:121–7.
Steinmetz CG, Xie P, Weiner H, Hurley TD. Structure of mitochondrial aldehyde dehydrogenase: the genetic component of ethanol aversion. Structure 1997;5:701–11.
Talfournier F, Pailot A, Stines-Chaumeil C, Branlant G. Stabilization and conformational isomerization of the cofactor during the catalysis in hydrolytic ALDHs. Chemico-Biological Interactions 2009;178:79–83.
Thoden JB, Holden HM, Wesenberg G, Raushel FM, Rayment I. Structure of carbamoyl phosphate synthetase: a journey of 96 A from substrate to product. Biochemistry 1997;36:6305–16.
Thoden JB, Huang X, Kim J, Raushel FM, Holden HM. Long-range allosteric transitions in carbamoyl phosphate synthetase. Protein Science 2004;13:2398–405.
Truong K, Su Y, Song J, Chen Y. Entropy-driven mechanism of an E3 ligase. Biochemistry 2011;50:5757–66.
Vedadi M, Meighen E. Critical glutamic acid residues affecting the mechanism and nucleotide specificity of *Vibrio harveyi* aldehyde dehydrogenase. European Journal of Biochemistry 1997;246:698–704.
Vellieux FM, Hajdu J, Verlinde CL, Groendijk H, Read RJ, Greenhough TJ, et al. Structure of glycosomal glyceraldehyde-3-phosphate dehydrogenase from *Trypanosoma brucei* determined from Laue data. Proceedings of the National Academy of Sciences of the United States of America 1993;90:2355–9.
Wang W, Baker P, Seah SYK. Comparison of two metal-dependent pyruvate aldolases related by convergent evolution: substrate specificity, kinetic mechanism and substrate channeling. Biochemistry 2010;49:3774–82.
Wang W, Seah SYK. Purification and biochemical characterization of a pyruvate-specific class II aldolase, HpaI. Biochemistry 2005;44:9447–55.
Wang X, Weiner H. Involvement of glutamate 268 in the active site of human liver mitochondrial (class 2) aldehyde dehydrogenase as probed by site-directed mutagenesis. Biochemistry 1995;34:237–43.
Weeks A, Lund L, Raushel FM. Tunneling of intermediates in enzyme-catalyzed reactions. Current Opinion in Chemical Biology 2006;10:465–72.
Yan R, Chen J. Coenzyme A-acylating aldehyde dehydrogenase from *Clostridium beijerinckii* NRRL B592. Applied and Environmental Microbiology 1990;56:2591–9.
Zhang L, Ahvazi B, Szittner R, Vrielink A, Meighen E. Change of nucleotide specificity and enhancement of catalytic efficiency in single point mutants of *Vibrio harveyi* aldehyde dehydrogenase. Biochemistry 1999;38:11440–7.